Supporting Information

Patterned tungsten disulfide/graphene heterostructures for efficient multifunctional optoelectronic devices

A. Rossi,[1,2] D. Spirito,[3] F. Bianco,[2] S. Forti,[1] F. Fabbri,[1] H. Büch,[1] A. Tredicucci,[2,4] R. Krahne[3,5] and C. Coletti[1,5]

1. Center for Nanotechnology Innovation @NEST, Istituto Italiano di Tecnologia, Piazza S. Silvestro 12, 56127 Pisa, Italy
2. NEST, Istituto Nanoscienze – CNR and Scuola Normale Superiore, Piazza San Silvestro 12, 56127 Pisa, Italy
3. Nanochemistry Department, Istituto Italiano di Tecnologia, Via Morego 30, 16163 Genova, Italy
4. Dipartimento di Fisica "E. Fermi", Università di Pisa, L.go Pontecorvo 3, 56127 Pisa, Italy
5. Graphene Labs, Istituto Italiano di Tecnologia, Via Morego 30, 16163 Genova, Italy

Raman characterization of as grown epitaxial graphene and WS2 on epitaxial graphene.

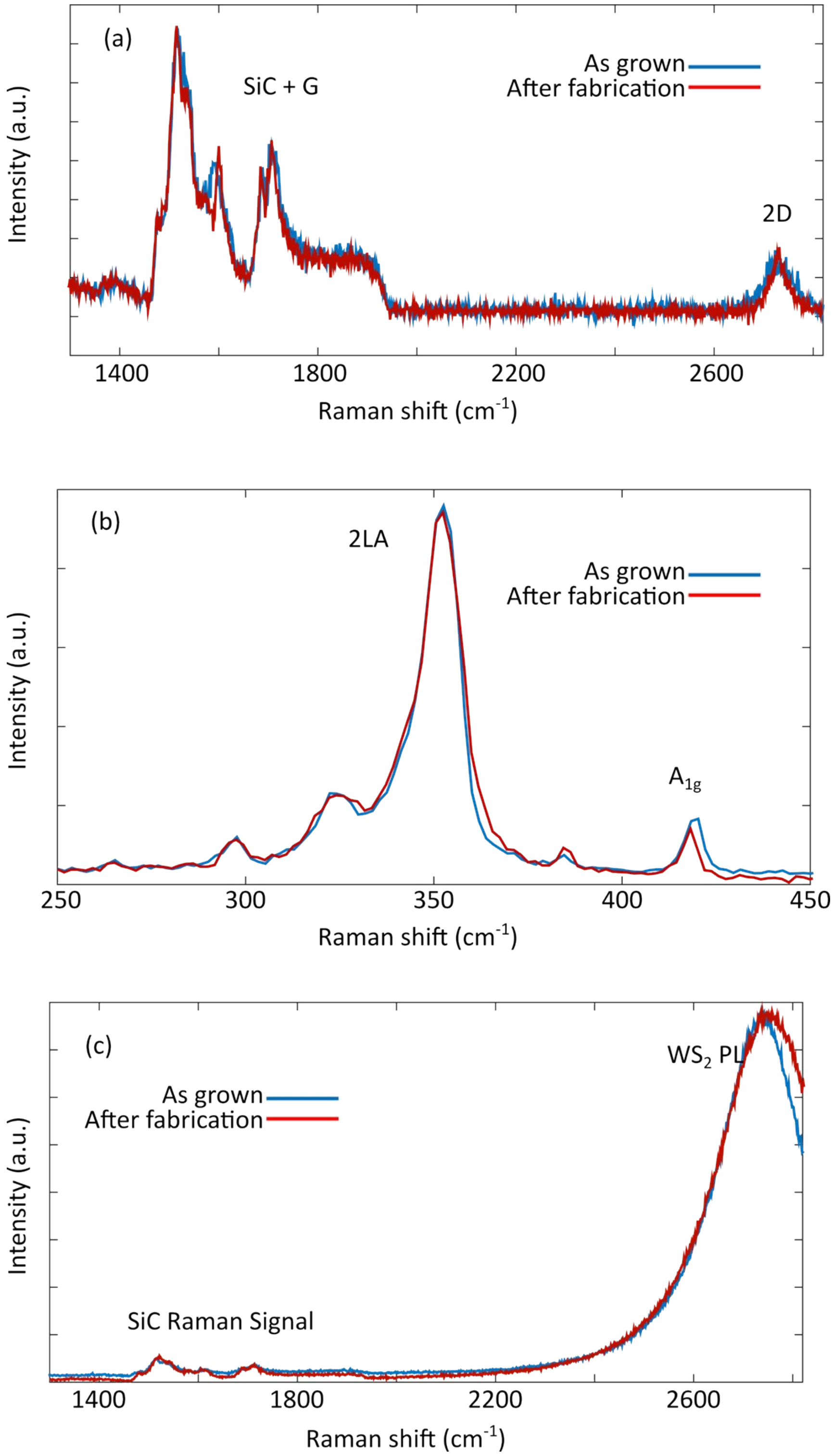

Fig. S1. Typical Raman spectra taken for as grown materials (blue) and after all fabrication steps (red) of (a) graphene and (b) WS_2. Panel (c) shows the PL emission of WS_2.

Raman and PL data of materials as-grown and after device fabrication are reported in Fig. S1. Blue curves are relative to as-grown materials and red curves are taken after the fabrication steps. The comparison of these spectra demonstrates that the WS_2 is not damaged by the fabrication steps, in fact the intensities and the width of both the 2LA and A_{1g} peaks remain unchanged. This result is also confirmed by the light emission analysis shown in panel (c) where the PL spectra before and after the fabrication process demonstrates that our fabrication steps does not induce any considerable change in the PL intensity, width and peak position, confirming that also the additional generation of point defects during the process is minimal. In the graphene areas (panel(a)) the 2D peak position and width in the spectra taken before and after the processing are similar, demonstrating no degradation of the crystalline quality of graphene due to the fabrication steps.

Structural characterization of WS_2

Raman analysis has been performed to test the homogeneity and quality of the sample. The measurement has been carried out using a laser power of 5mW with a 100x magnification objective and 532 nm wavelength. Fig. S2(a) reports the ratio of the two main peaks of WS_2. The map shows the transition from bilayer to monolayer moving from the contacts towards the center of the channel. This is compatible with the fact that the mask edges (now replaced by metallic contact) act as nucleation points. Fig. S2(b) reports the map relative to the A_{1g} peak width. The uniformity of the width indicates the high crystal quality of WS_2 layer. Fig. S2(c) display a representative WS_2 spectrum collected in the channel.

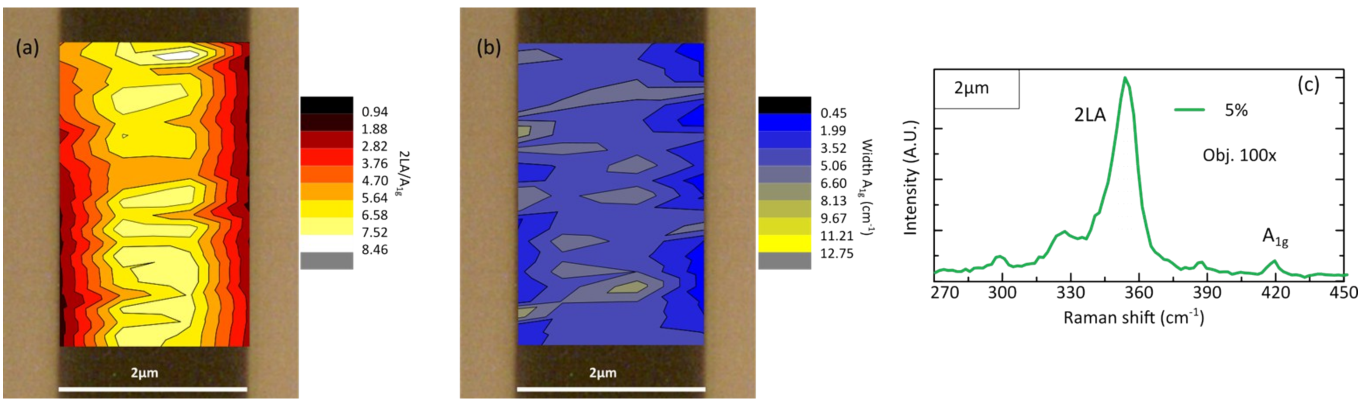

Fig. S2. (a) Raman map of 2LA/A1g ratio peak intensity over the device channel. (b) Raman map of A1g peak width. (c)Representative WS2 spectrum of the investigated area.

AFM analysis of WS2/graphene and graphene only areas

In Fig. S3 a representative AFM topography image taken over an area which includes both graphene and WS_2/graphene is reported. The scan is taken prior to contact deposition and after mask removal. The graphene area is clearly residue free (zoom-in on the left), with a root mean square (RMS) roughness of 448 pm. Fabrication residues are present on the WS_2 area and absent on the graphene portion, which is covered by the gold mask until the end of the process. A few WS_2 bilayer crystals are visible close to where the mask edge was placed. This finding is in agreement with what retrieved via Raman analysis and attributed to the favorable seeding caused by the mask itself during WS_2 growth.

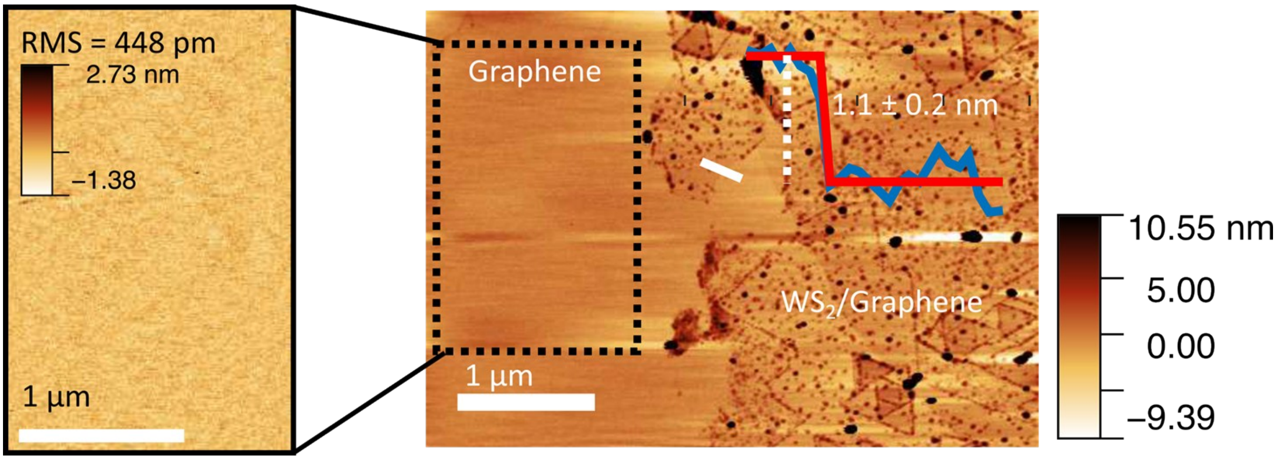

Fig. S3. Topography obtained via AFM scan in tapping mode of the area at the interface between WS2/graphene and graphene only area. The blue line is the line profile taken along the white dashed line (i.e., across WS2 and graphene). The red line represents the fit of the obtained curve.

I/V curve of WS_2 and Gr-only devices

Device contacts are tested measuring I/V curves with no illumination.

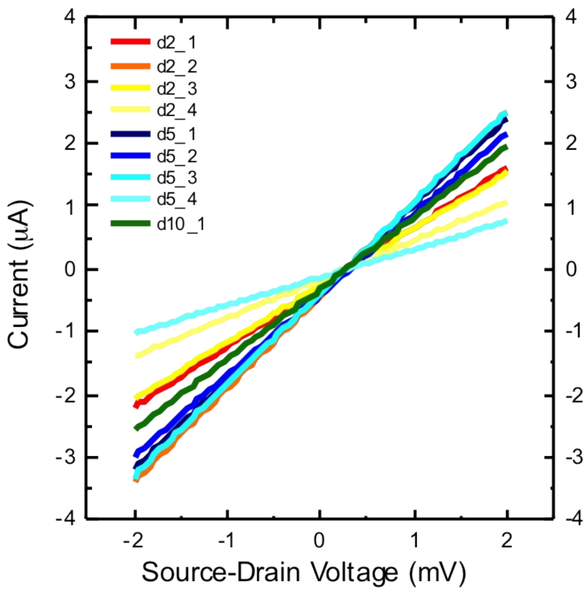

Fig. S4. I/V curves for WS2/Gr and Gr-only devices. d2, d5 and d10 curves are for devices with channel length of 2 µm, 5 µm and 10 µm respectively. Devices number 1,2,3 are WS2/Gr based and number 4 Gr-only.

I/V curves are reported in Fig. S4 for all devices including the ones with no WS_2. All devices show a linear dependence, thus indicating good ohmic contacts. The resistance obtained from the curves varies from 1 to 2 kΩ, which includes the contributions from the contact resistance and sheet resistance. Transfer Length Measurements (TLM) are reported in Fig. S5 and allow for extracting an effective contact resistivity of $(1.35 \pm 0.08) \times 10^4\ \Omega \cdot \mu m$. Measurements have been performed in air at room temperature. The devices analyzed are the same used for photocurrent measurements reported in this work, with channel lengths of 2, 5 and 10 µm.

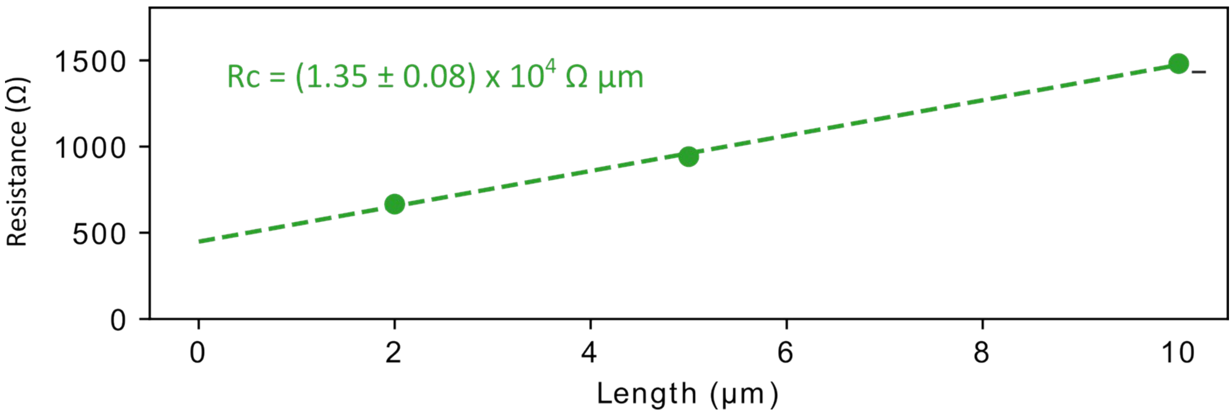

Fig. S5. Transfer Length Measurement performed for the WS_2/graphene devices studied in this work.

Photoresponsivity of Gr-only devices

Devices made using only graphene as active channel have been investigated to compare their performances with respect to those of the hybrid heterostructures. The measured responsivity is R~0.04 A/W, obtained with 638 nm wavelength excitation, bias voltage V_B = 2 V, optical modulation frequency set at 23 Hz and light intensity 250 mW/cm^2. The correspondent value obtained for the detectivity is $D^* = 5.2 \times 10^5\, Jones$.

DC measurement of photocurrent under blue light at 473 nm

Photocurrent is measured in DC mode using blue light. The measurement is taken over long time scale (more than 1hr). In this range the WS_2/graphene device displays a persistent photo current (PPC) with no appreciable damping (panel(a)). The same behavior is displayed for graphene-only devices, confirming that this feature is not due to the WS_2/Gr interface (panel(b)).

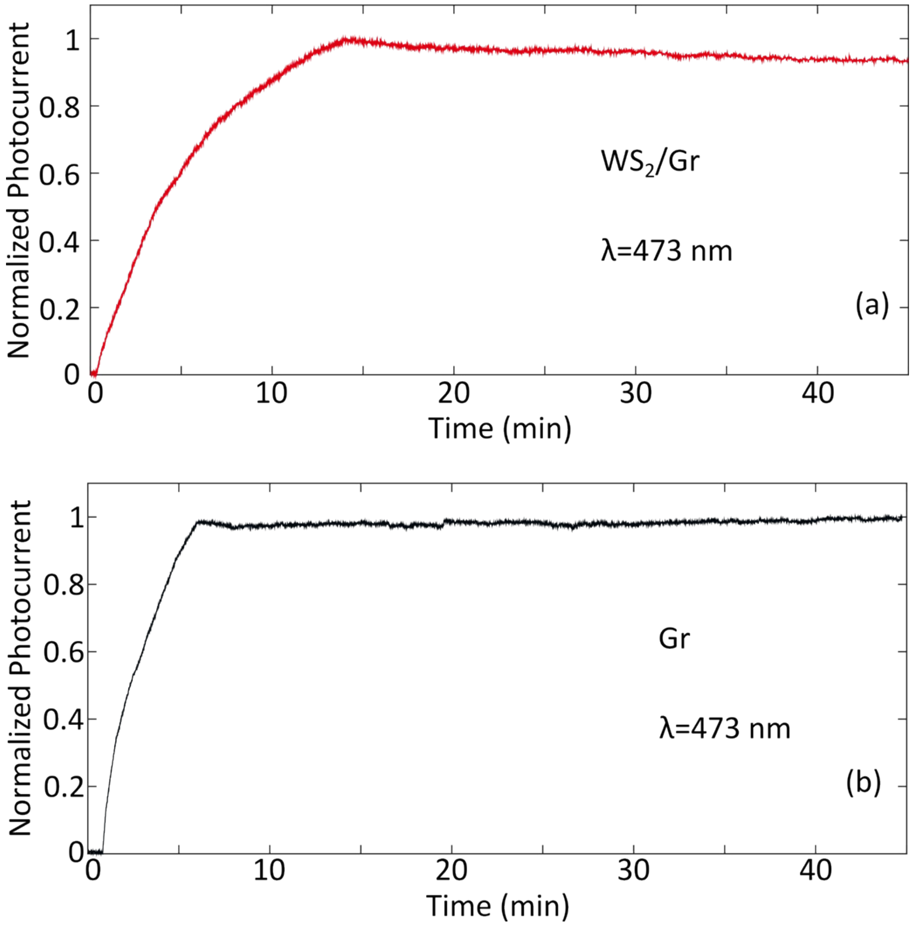

Fig. S6. DC photocurrent measurements vs time for WS2/graphene(a) and Gr-only (b) device under 473 nm light irradiation at bias voltage VB=1.8 V.

DC measurement of photocurrent in 10μm devices to exclude contact contributions

To exclude any contribution from the electrode contacts to the photocurrent, a DC measurement is carried out with a light spot size small enough to exclude illumination of the gold structures. The measurement is performed on three devices having 10μm channel length. Using a 100x magnification objective, the spot size is 1 μm in diameter. The PCC is present also in this case in all three devices. Therefore it is possible to exclude any role played by contacts.

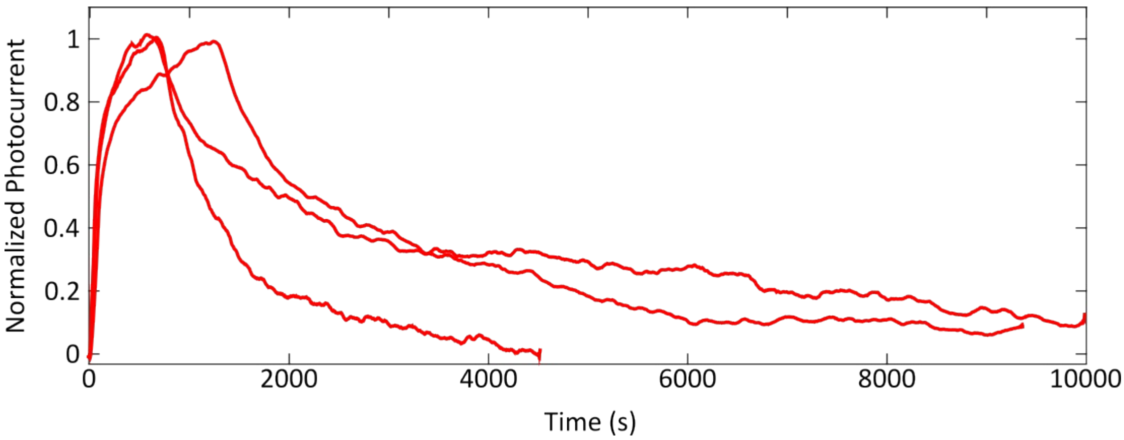

Fig. S7. DC photocurrent measurement vs time, under 532 nm light irradiation on devices with a channel length of 10μm at bias voltage V_B=1 V and incident power of 10 mW. The diameter of the laser spot is ~1 μm.